4 Kelvin Regenerator Loss Measurements

R. Taylor[1,2], M. Lewis[2], and R. Radebaugh[2]

[1]Department of Mechanical Engineering
Virginia Military Institute
Lexington, VA 24450 USA

[2]Material Measurement Laboratory
National Institute of Standards and Technology
Boulder, CO 80305 USA

ABSTRACT

Past work has described a NIST three-stage regenerator test facility for validation of predictive regenerator models over a temperature range of 30-4 K. This test facility is unique as the regenerator loss for a given configuration can be measured over a wide operational space that includes the ability to modulate the cold end test temperature from 3-7 K, warm end test temperature from 18-30 K, charge pressure from 1-2 MPa, and cold end phase angle from 0° to -45°. However, a drawback with the original design involved the inability to isolate the various losses in the regenerator for specific conditions. Experimental isolation of the dominant losses in a 4 K regenerator is critical for higher-order predictive model validation and development of next-generation regenerator designs.

In normal operation, the dominant losses in a 4 K regenerator stem from imperfect matrix-gas heat transfer (ineffectiveness loss) and a non-ideal gas working fluid (real gas loss). Of these two losses, the real gas loss is unique as it can turn into a gain under specific operating conditions. Practically, isolating these two losses experimentally is no trivial task. This work presents an experimental method to isolate the ineffectiveness and real gas loss terms. In development of the experimental method, a detailed discussion of the thermal loads and enthalpy flows in the regenerator and secondary heat exchanger components is presented. Real gas effects near the critical point of ^{4}He are analyzed and discussed using a simple thermodynamic analysis. Based on this analysis, the non-dimensional volume expansivity is used to determine the real gas enthalpy flow directions and resulting thermal loads. Additionally, physical implementation of the revised experimental techniques in the NIST facility is discussed along with measurement redundancy for investigation of experimental error.

INTRODUCTION

Modern, high-frequency, Pulse Tube Cryocooler (PTC) systems represent a practical method for attaining cryogenic temperatures (3.5-120K). In recent memory, focus on performance improvements has been plentiful yet actual performance improvements have somewhat lagged. This is especially true for 4K applications that range from cooling of

Cryocoolers 18, edited by S.D. Miller and R.G. Ross, Jr.

superconducting electronics to replacement of liquid cryogens for laboratory settings. Furthermore, while PTC technology has been commercialized (GM variant) by various manufacturers for nominal cold end temperatures of 4.2K, wide use of high-frequency systems is lacking except for aerospace and defense applications. The advantages of high-frequency PTC technology relative to current low-frequency GM technology include higher cooling density, smaller physical size, and potentially more reliable operation due to flexure bearing linear compressors. While the advantages for high-frequency systems are numerous, a plethora of issues ranging from phase shifting to individual component losses exist that have prevented high-frequency systems from outperforming GM variants. In parallel, future 4K cooling applications will require even higher cooling density, smaller physical size, and reliability surpassing present technology.

To advance 4K high-frequency PTC technology, a thorough understanding of the complex losses is required to enable enhanced system performance. The relative magnitude of PTC losses considering entropy generation is shown in Figure 1 for two conditions: a moderate cold end temperature of 80K and a cold end temperature of 4K. The data in Figure 1 show a significant difference in the magnitude of losses for the 4K and 80K cases. For operation at 4K, the dominant losses for a PTC system are the real gas pressurization loss and the regenerator ineffectiveness loss. This is in contrast to the 80K case where the real gas loss is minimal and the primary losses are attributed to the regenerator ineffectiveness and the pulse tube losses. Specifically, at moderate cryogenic temperatures, the pulse tube loss is comparable in magnitude to the regenerator ineffectiveness loss while the real gas loss is minor. For 4K regenerators, this trend is reversed and the real gas loss dwarfs the ineffectiveness loss while the pulse tube loss is relatively small.

To enhance understanding of the complex loss phenomena in high frequency 4K regenerators, and to optimize and enhance performance, various predictive modeling programs are used. In general, these models include SAGE[1] (overall system), REGEN3.3[2] (regenerator), and commercial CFD codes (overall or component based). While modeling is clearly the ideal manner through which optimization is attained when compared to costly experimental hardware, lack of validation data for a temperature range of 4-30K leaves questions regarding the validity of modeling results in this complex hydrodynamic and thermal regime. Furthermore, the relative magnitude of the losses is required for systemic predictive model validation. Generally, model validation has been achieved using bulk measurements of compressor input power, cooling, power, and heat rejection. Using these measured quantities it is relatively easy to provide relative magnitudes for bulk losses in the regenerator and pulse tube components. However, for validation of highly advanced predictive models for 4-30K regenerators, isolation and accurate measurement of the dominant losses becomes critical and necessary. This paper specifically addresses this issue in the context of a 4K NIST regenerator test facility and associated techniques and analyses for isolation of dominant high frequency regenerator losses for temperatures from 4-30K.

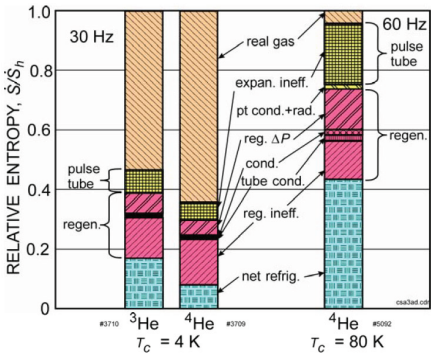

Figure 1: Illustration showing the relative magnitude of losses in a PTC with delineation of the regenerator and pulse tube losses; from Radebaugh[3].

NIST 4 KELVIN REGENERATOR TEST FACILITY DESIGN

Previous work by the authors[4] has detailed a three-stage regenerator test facility. This test facility is designed for a wide operational space with measurements possible from 3.2-100K. Features specific to 4K regenerator testing are summarized below:

4K Testing Conditions

1) Off-axis measurements from 0° → 180°,
2) Operating frequency from 30 Hz → 40 Hz,
3) Charge pressure of 0.75 MPa → 1.5 MPa,
4) Cold end phase angle from 0° → -45°,
5) Regenerator cold end temperature variation from 3.2K → 7K, and
6) Regenerator warm temperature variation from 20K → 35K

The nominal NIST test facility configuration is shown graphically in Figure 2. The primary system components shown in Figure 2 include: linear compressor, aftercooler, 1st stage pre-cooling regenerator, 1st stage thermal intercept, 2nd stage pre-cooling regenerator, 2nd stage thermal intercept, 3rd stage test regenerator or test regenerator and pulse tube, 3rd stage thermal intercept, and a cold expander. A commercial GM cryocooler provides precooling at the first and second stage intercepts which operate at nominal temperatures of 80K and 20K, respectively. The test regenerator cold end (3rd stage thermal intercept) is fixed at a nominal temperature of 4.2 K using LHe with modulation occurring via trim heaters and a vacuum pump. Cooling the 3rd stage thermal intercept using LHe was implemented for wide load acceptance capacity, and the large specific heat of the boil-off He gas allows for supplemental cooling of the cold expander and radiation shields. Unique to this test facility is the ability to modulate the phase angle between pressure and flow in real time. This ability is achieved using a small linear compressor that operates as a frequency-locked cold expander. Previous work by the authors[5] has shown this expander to be capable of sustained operation at cryogenic temperatures below 30K. Furthermore, the developed test facility allows for a high degree of testing flexibly due to its modular nature. This allows for easy hardware interfacing and can be readily instrumented for measurement of pulse tube energy flows.

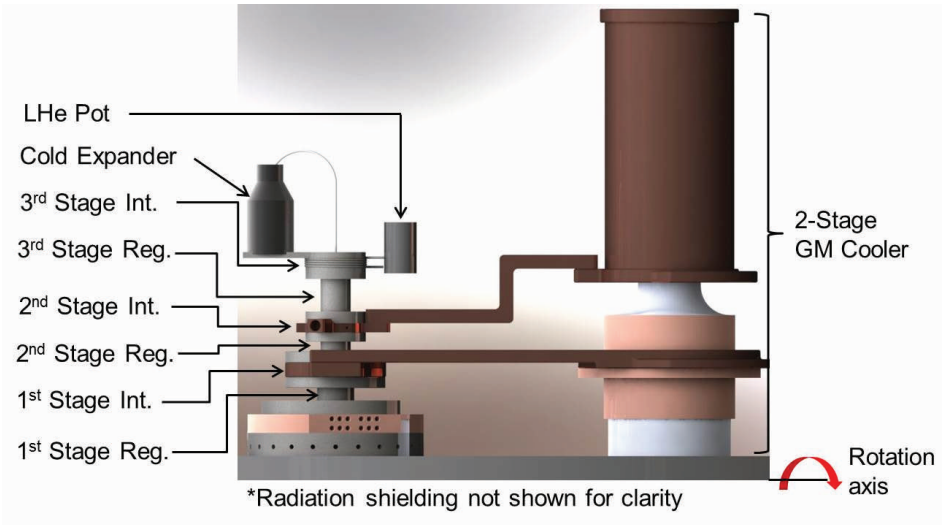

Figure 2: Illustration of the NIST 4 Kelvin regenerator test facility with major components noted.

4 KELVIN REGENERATOR ENERGY FLOWS

To aid development of an isolated loss measurement methodology and associated experimental hardware, a fundamental analysis of the thermal loads and enthalpy flows for a regenerator operating from 4-30K is required. For the analyses presented in this section, conduction terms are neglected due to magnitude. In practice, a parasitic conduction loss does occur and manifests as a thermal load serving to reduced available refrigeration. The basis for the analyses presented in the reminder of this section is a regenerator that is operating under conditions consistent with 4K cooling. Located at each end of the regenerator is an isothermalizer. The isothermalizer is used to damp out dynamic temperature changes entering the regenerator during the warm and cold blow processes. Upstream of the warm isothermalizer is the compressor or upper stages in a multi-stage cooler. The temperature of this space is the same temperature as the warm isothermalizer. Downstream of the cold isothermalizer is the expansion space (cold expander) that is maintained at the same temperature as the cold isothermalizer. For consistency, flows from warm to cold and thermal inputs have a positive value.

Case 1 – Perfect Regenerator, Ideal Gas

Analysis of a basic regenerator operating between prescribed temperature limits is readily performed if the regenerator is assumed perfect and the working fluid is an ideal gas. This case is illustrated in Figure 3a. In this ideal case, no thermal loads are added or removed from the system. Specifically, at the warm isothermalizer, there exists no enthalpy flow from upper stages or any thermal communication with the surroundings. Similarly, at the cold isothermalizer, there exists no enthalpy flow from expansion space or any thermal communication with the surroundings. In this limited case, the time-averaged enthalpy flow in the regenerator component must be zero. This result is physically intuitive as no dynamic temperatures exist anywhere in the regenerator eliminating the ineffectiveness loss and the enthalpy of the working fluid enthalpy is dependent only on temperature.

Case 2 – Imperfect Regenerator, Ideal Gas

In practice, all regenerators have imperfect heat transfer between the working fluid and the porous matrix. This case is similar to that of Case 1 and is illustrated in Figure 3b. Due to the imperfect heat transfer manifesting as the ineffectiveness loss, a dynamic temperature develops in the regenerator resulting in a time-averaged enthalpy flow from the warm to cold end. As a result, and based on energy conservation for the regenerator component, thermal energy equal to

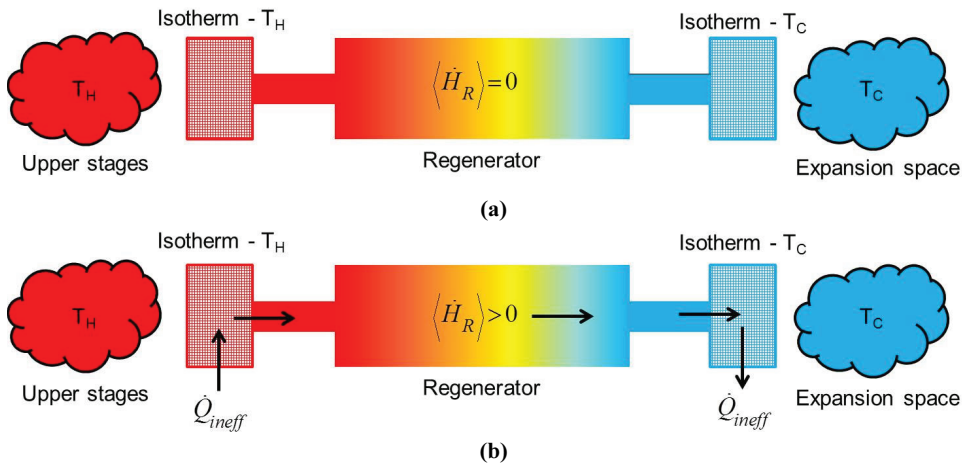

Figure 3: Illustration showing thermal loads and enthalpy energy flows for (a) a perfect regenerator with an ideal gas working fluid, and (b) an imperfect regenerator with an ideal gas working fluid.

the time-averaged enthalpy flow must be absorbed at the warm isothermalizer and is subsequently rejected as a thermal load at the cold isothermalizer. No other enthalpy flow terms are present due to elimination of dynamic temperature at the isothermalizers. The direction of the ineffectiveness loss can be shown mathematically using a time-averaged energy balance applied to the warm isothermalizer as shown in Eqn. 1,

$$\begin{aligned} &\dot{Q}_{ineff} = \oint \left[\dot{m}h(T_H)\big|_{out} - \dot{m}h(T)\big|_{in} \right] dt \\ &\text{when } \dot{m} \text{ is positive, } 0 = \oint \left[\dot{m}h(T_H)\big|_{out} - \dot{m}h(T)\big|_{in} \right] dt \;\; as \;\; T_H = T \\ &\text{when } \dot{m} \text{ is negative, } 0 < \oint \left[\dot{m}h(T_H)\big|_{out} - \dot{m}h(T)\big|_{in} \right] dt \;\; as \;\; T_H > T \end{aligned} \tag{1}$$

The analysis in Eq. 1 illustrates that the time-averaged enthalpy flow at the warm isothermalizer flows toward the cold isothermalizer and is equal to the added thermal load. This analysis can also be applied to the cold isothermalizer which yields the opposite effect; enthalpy flows into the cold isothermalizer and is rejected as a thermal load. In this case, the regenerator ineffectiveness loss can be measured at either the warm or cold isothermalizer. Practically this occurs by measuring the thermal input required to maintain the warm isothermalizer at T_H or measure the heat rejection at the cold isothermalizer for a specific T_C.

Case 3 – Perfect Regenerator, Real Gas

For moderate cryogenic temperatures, the working fluid may be readily approximated as an ideal gas for which h = *f*(T). However, the ideal gas assumption breaks down for regenerators that operate in the temperature range of 4-30K and real gas effects must be considered. This is due to the enthalpy of the working fluid between 4-30K becoming pressure dependent yielding h = *f*(T,P). Practically, real gas properties cause a time-averaged enthalpy flow to develop in the regenerator. The problem with this enthalpy flow stems from the direction being dependent on the combination of temperature and pressure. To fully analyze the real gas enthalpy flow, a perfect regenerator with a real gas working fluid is considered and illustrated in Figure 4. Observation of Figure 4 shows a marked difference when compared to Cases 1 and 2. In this case, a thermal load may arise at either isothermalizer and more important, enthalpy may flow to/from the upper stage or expansion space. Unlike Case 1 and 2 in which these terms were zero based on elimination of dynamic temperature, now these terms are non-zero due to the enthalpy having pressure dependence. Criteria must be developed considering temperature and pressure via real gas thermodynamics to ascertain the direction of the real gas enthalpy flows.

Real Gas Thermodynamics

Directional dependence of the real gas enthalpy flow terms noted in Figure 4 can be readily determined by analyzing, in this case, a cold expander (expansion space). Analysis of the cold expander focuses on the relationship between heat and work. The gas volume in the expander undergoes a pressure change during a reversible, isothermal process. For this process, the differential heat which is also the refrigeration capacity, dQ_r is expressed in Eqn. 2,

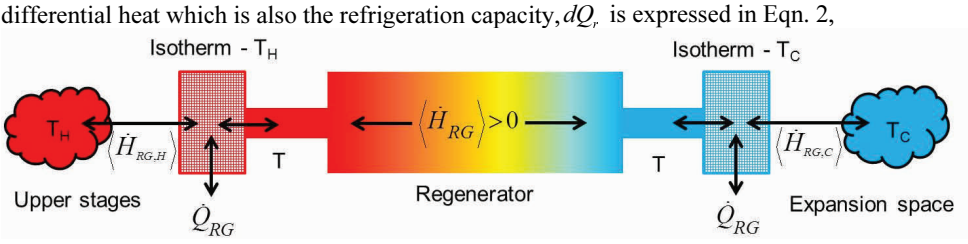

Figure 4: Illustration showing thermal loads and enthalpy flows for a perfect regenerator with a non-ideal gas working fluid. Ambiguity stems from the direction of the real gas flow.

$$dQ_r = TdS = T\left[\left(\frac{\delta S}{\delta T}\right)_P dT + \left(\frac{\delta S}{\delta P}\right)_T dP\right] = T\left(\frac{\delta S}{\delta P}\right)_T dP \tag{2}$$

In Eqn. 2, the first partial derivative term is zero as the process is isothermal. The resulting expression relates the differential heat to the partial entropy with respect to pressure at constant temperature. However, the final expression in Eqn. 2 is not very intuitive but can be recast into a more intuitive form using Maxwell's relations, the volume expansivity, and the definition of expansion work,

$$-\left(\frac{\delta S}{\delta P}\right)_T = \left(\frac{\delta V}{\delta T}\right)_P \tag{3}$$

$$\beta = \frac{1}{V}\left(\frac{\delta V}{\delta T}\right)_P \tag{4}$$

$$dW_{exp} = -VdP \tag{5}$$

Combining Eqns. 2-5 yields an expression relating the differential heat to differential work,

$$dQ_r = T\beta\, dW_{exp} \tag{6}$$

where dW_{exp} is the expander work output, T is the gas temperature, and β is the volume expansivity of the working fluid. The expression in Eqn. 6 is very simple yet highly informative due to the product $T\beta$. Herein this term is referred as the non-dimensional volume expansivity coefficient and it readily captures the working fluid real gas effects as shown in Figure 5. In the limiting case of an ideal gas, $T\beta$=1 and the refrigeration load accepted is output as expansion work. However, as shown in Figure 5 for real gases, $T\beta$ deviates significantly from 1 when approaching the critical point for ^{4}He. Observation of Eqn. 6 coupled with the deviation of $T\beta$ near the critical point leads to two interesting observations:

1. For $T\beta > 1$, $dQ_r > dW_{exp}$ indicating the refrigeration capacity is enhanced and the real gas enthalpy flow is from the expansion space to the upper stage,
2. For $T\beta < 1$, $dQ_r < dW_{exp}$ indicating the refrigeration capacity is reduced and the real gas enthalpy flow is from the upper stage to the expansion space.

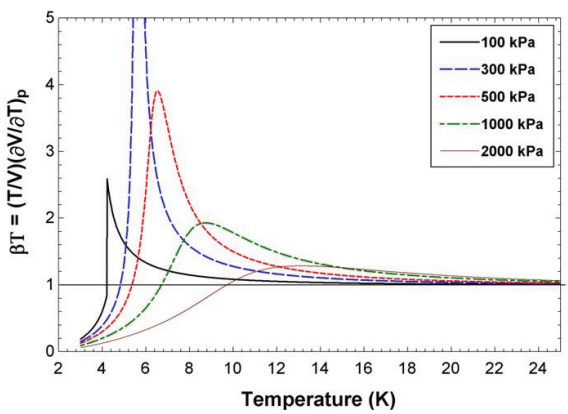

Figure 5: Illustration showing the behavior of the non-dimensional volume expansivity for ^{4}He at temperatures near the critical point for various pressures. The temperature range selected is aligned with the normal operating range for a 4K regenerator.

Using this information coupled with Figure 5 for selected operating pressures and cold and warm temperatures, the direction of the real gas terms in Figure 4 may be determined. However, the thermal addition or rejection due to the enthalpy imbalance between the two real gas flows must be determined. Determination of this heat loading can be determined by considering the fluid capacitance during the warm blow and cold blow processes. This process is the AC analog of the common DC flow minimum capacitance analysis used for recuperative heat exchangers. In this regard, and based on the enthalpy as a function of temperature and pressure, the blow process with the minimum enthalpy is computed. Based on the blow process with the minimum enthalpy change, the excess enthalpy in the alternate stream must either be removed or added dependent on flow direction. As such, the relationship between $T\beta$ evaluated at the warm and cold ends may be correlated to the stream with minimum capacitance and whether energy is lost or gained at the isothermalizers. Based on the analysis, the following criteria were developed in terms of evaluation of $T\beta$ using the regenerator end temperatures and the mean operating pressure,

1. High Pressure Case - $T\beta_C < T\beta_H$, the warm blow process is capacitance limited resulting in a thermal load being added at the warm isothermalizer,
2. Low Pressure Case - $T\beta_C > T\beta_H$, the cold blow process is capacitance limited resulting in a thermal load being rejected at the cold isothermalizer,

Physical realization of these two cases is illustrated in Figure 6. Observation of Figure 6a shows the low-pressure case in which the cold blow process is capacitance limited. In this case, the warm blow process is unable to accept excess thermal loading from the real gas flow at the cold end. Due to this limit a thermal load $\dot{Q}_{RG}$, equal to the difference between the cold and warm real gas flows, is rejected at the cold isothermalizer. This results in a net real gas enthalpy flow through the regenerator equal to the warm real gas enthalpy flow. The direction of this enthalpy flow is from cold to warm and there exists no thermal load at the warm isothermalizer. In contrast, Figure 6b shows the high-pressure case in which the warm blow process is capacitance limited. In this case, the cold blow process has excess enthalpy that must be balanced at the warm isothermalizer. Due to this limit a thermal load $\dot{Q}_{RG}$, equal to the difference between the cold and warm real gas flows, must be added at the warm isothermalizer. This results in a net real gas enthalpy flow through the regenerator equal to the cold real gas enthalpy flow. The direction of this enthalpy flow is from warm to cold and there exists no thermal load at the cold isothermalizer.

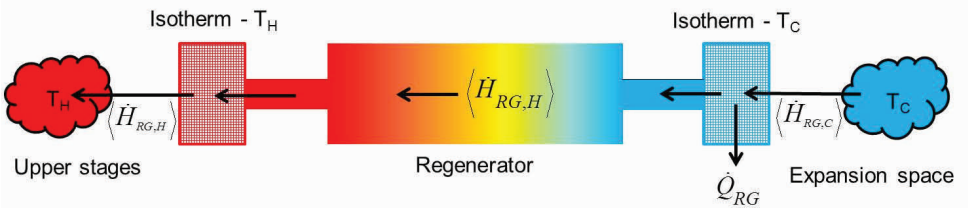

(a) Low pressure case

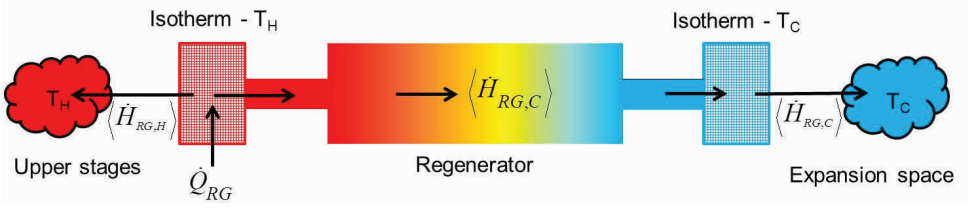

(b) High Pressure Case

Figure 6: Illustration showing the thermal loads and enthalpy flow directions for perfect regenerator and real gas for (a) the low pressure scenario, and (b) the high pressure scenario.

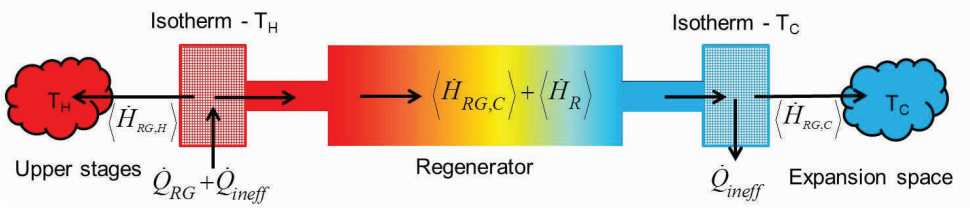

Figure 7: Illustration showing thermal loads and enthalpy flows for an imperfect regenerator with a non-ideal gas working fluid when the mean system pressure is high.

Case 4 – Imperfect Regenerator, Real Gas

Observation of cases 1-3 yields specific information in terms of isolated limits. In practice, a normal regenerator operating between the temperature limits of 4-30K is aligned with a combination of cases 2 & 3. More specifically, due to operational pressure in modern high-frequency PTC systems equaling or exceeding 500 kPa, the most applicable combination is case 2 with the high-pressure variant of case 3. Representation of this condition is illustrated in Figure 7. Observation of Figure 7 shows the combination of the enthalpy and energy flows for these two cases. Of note is the energy flow associated with the regenerator ineffectiveness remains consistent with the direction and thermal loading discussed for the high pressure scenario in case 3. The net result is a total regenerator enthalpy flow towards the cold end that is consistent with the sum of the ineffectiveness enthalpy flow and the real gas enthalpy flow. In terms of decoupling the regenerator and real gas losses, this situation is ideal. As the only enthalpy flow that may flow towards the expander is due to the real gas enthalpy flow, the sole thermal load at the cold isothermalizer is due to the regenerator loss. Physical measurement of the two decoupled losses now becomes possible using this scenario.

4 KELVIN REGENERATOR LOSS MEASUREMENTS

Physical isolation and measurement of the ineffectiveness and real gas regenerator losses is performed by transforming the high-pressure analysis shown in Figure 7 into a physical hardware representation as shown in Figure 8. Observation of Figure 8 in relation to Figure 7 shows two major changes: 1) two cold isothermalizers are used, and 2) the expansion space is represented by an actual cold expander. The use of two cold isothermalizers enables redundancy in the real gas loss measurement and allows for regulation of the expander temperature. Use of a cold expander serves two purposes: 1) the expander is used to set the desired phasor relationship at the regenerator cold end during testing, and 2) is used to facilitate the redundant measurement of the real gas loss.

A more detailed basis for measuring the two losses, primary and redundant, is presented in Figure 9. Measurement of the regenerator ineffectiveness loss is performed at the first cold isothermalizer as shown in Figure 9a. In this case, the total time-averaged enthalpy flow that enters the isothermalizer is the combination of the ineffectiveness loss and the real gas loss. A thermal load equal to the regenerator ineffectiveness loss is rejected to a thermally linked LHe pot. Knowledge of the thermodynamic condition of the LHe is readily determined with pressure

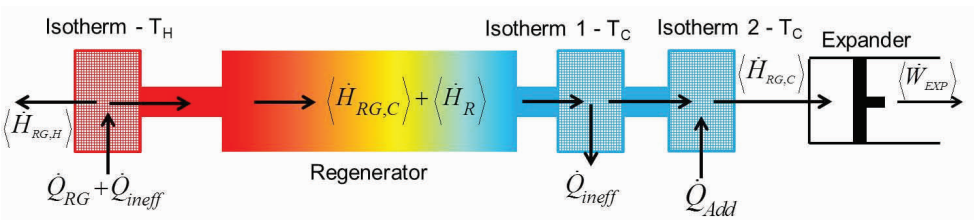

Figure 8: Illustration showing the physical hardware implementation for measurement of the delineated regenerator losses.

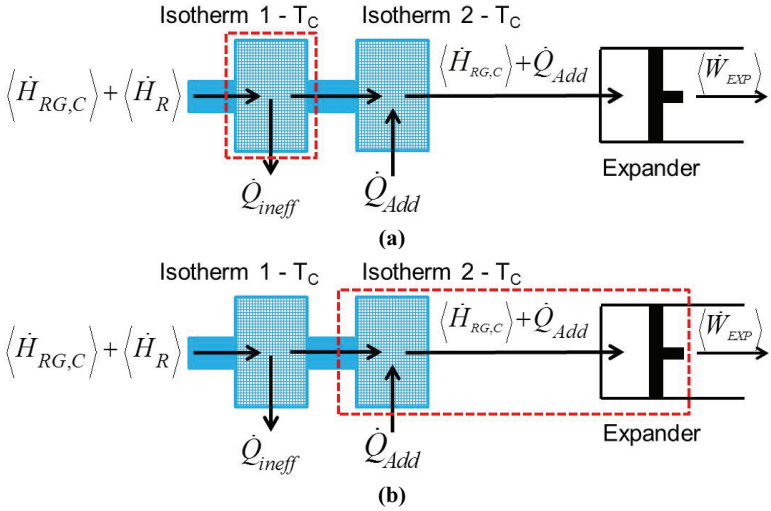

Figure 9: Illustration showing the energy balance and relevant enthalpy flows and thermal loads for a control volume consisting of (a) the first cold isothermalizer system, and (b) the second isothermalizer – expander combined system.

measurement in the LHe pot. Measurement of the LHe boil off rate is accomplished at room temperature by passing the gas through an ice-bath and then through a precision mass flow meter. Using this information, the thermal load rejected at this isothermalizer is computed and equal to the ineffectiveness loss for the given operating conditions. It should be noted that the only thermal load that may be rejected at this location is due to ineffectiveness as the excess temperature has no real gas component. This is due to the warm blow process being capacitance limited. Isolation and measurement of the real gas enthalpy flow is achieved by recording the instantaneous pressure and mass flow waveforms at the exit of the first isothermalizer using standard pressure transducers and mass flow calibration curves. Using the measured waveforms, the time-averaged real gas enthalpy flow is computed using numerical integration. It should be noted that conduction losses are calibrated out in advance.

To enable confidence in the measurement of the real gas loss, a secondary and redundant set of measurements are performed as illustrated in Figure 9b. In this case, the measurement system consists of two components; the second isothermalizer and the cold expander. During normal operation, the real gas enthalpy flows to the expander and reduces but does not eliminate the cooling power generated by the expander. As a result, the second isothermalizer attains a lower temperature than the first isothermalizer. To maintain both isothermalizers and the expander at a uniform temperature, heat is added using a standard resistance heater at the second isothermalizer. This heat is adjusted using a commercial PID controller to maintain the desired testing temperature. In addition, the expander power output is computed using normal electrical measurements. Note that expander ohmic heating is known and accounted for based on previous measurements[5] of the DC and AC resistance of the expander. Using the energy balance shown in Figure 9b, coupled with knowledge of the time-averaged expander power and the added thermal load, the real gas enthalpy entering the second isothermalizer is determined resulting in a redundant measurement of the real gas enthalpy flow. Comparing the real gas enthalpy flow determined using the analysis on the first isothermalizer and the analysis of the second isothermalizer – expander combination should yield equivalent results within experimental error. Large deviations would indicate systemic measurement errors. It should be noted that conduction losses are calibrated out in advance.

CONCLUSION

This paper has reviewed a NIST 4K regenerator test facility that allows for a unique and important testing capability that does not currently exist anywhere in the world. As part of the design verification and evaluation of the utility of the experimental measurements, it was deemed critical and necessary to develop an experimental methodology to isolate and measure the dominant losses in a regenerator operating in the temperature range of 4-30K. As part of this process, a real gas thermodynamic analysis was used along with flow capacitance information to determine the direction and thermal loads resulting from real gas effects. The analysis yielded criteria for performing regenerator loss measurements in which the regenerator ineffectiveness loss is isolated at a cold isothermalizer as a thermal rejection. The real gas loss is determined separately using measured waveforms for pressure and mass flow rate at the exit of the isothermalizer. Furthermore, redundancy is built-in to the real gas loss measurement through analysis of a second system that includes an additional cold isothermalizer and a cold expander. Using the new methodology, modifications to the experimental hardware for the NIST 4K facility were presented.

Current and continuing work is focused on assembly and verifying the performance of the two pre-cooling stages. During this process the 4K stage hardware, to include an additional isothermalizer, will be finalized and fabricated. Following completion of fabrication, assembly of the testing stage components will be performed. After successful assembly, calibrations will be performed and performance verified. Initial experimental measurements will focus on regenerators using GOS, Er50-Pr50, combinations of these two materials, and advanced regenerator matrix designs. The experimental measurements will be used to benchmark programs such as REGEN3.3 and other higher order models using CFD.

REFERENCES

1. Gedeon, D., “SAGE,” Gedeon Associates, Athens, OH, 2011.
2. Gary, J., O’Gallagher, A., Radebaugh, R., Huang, Y., and Marquardt, E., “REGEN3.3: User Manual,” National Institute of Standards and Technology, 2008.
3. Radebaugh, R., Huang, Y., O’Gallagher, A., and Gary, J., Optimization Calculations for a 30Hz, 4K Regenerator with Helium-3 Working Fluid, IEEE/CSC & ESAS European Superconductivity News Forum (ENSF), No. 1218, October 2010. pp. 1581-1592.
4. R. Taylor, M.A. Lewis, P.E. Bradley, and R. Radebaugh, “Development of a 4 K Regenerator and Pulse Tube Test Facility,” *Cryocoolers 17*, ICC Press, Boulder, CO (2012), pp. 219-228.
5. M.A. Lewis, P.E. Bradley, and R. Radebaugh, “Experiments with Linear Compressors for Phase Shifting in Pulse Tube Cryocoolers,” AIP Conf. Proc. 1573 (2014), pp. 562-569.